Structure and catalytic mechanism of glucosamine 6-phosphate deaminase from *Escherichia coli* at 2.1 Å resolution

Glaucius Oliva[1], Marcos RM Fontes[1†], Richard C Garratt[1], Myriam M Altamirano[2], Mario L Calcagno[2] and Eduardo Horjales[1‡*]

[1]Instituto de Fisica de São Carlos, Universidade de São Paulo, São Carlos, SP, 13560–970, Brazil and [2]Departamento de Bioquímica, Facultad de Medicina, Universidad Nacional Autónoma de México, 04510, México, D.F., Mexico

Background: Glucosamine 6-phosphate deaminase from *Escherichia coli* is an allosteric hexameric enzyme which catalyzes the reversible conversion of D-glucosamine 6-phosphate into D-fructose 6-phosphate and ammonium ion and is activated by *N*-acetyl-D-glucosamine 6-phosphate. Mechanistically, it belongs to the group of aldose-ketose isomerases, but its reaction also accomplishes a simultaneous amination/deamination. The determination of the structure of this protein provides fundamental knowledge for understanding its mode of action and the nature of allosteric conformational changes that regulate its function.

Results: The crystal structure of glucosamine 6-phosphate deaminase with bound phosphate ions is presented at 2.1 Å resolution together with the refined structures of the enzyme in complexes with its allosteric activator and with a competitive inhibitor. The protein fold can be described as a modified NAD-binding domain.

Conclusions: From the similarities between the three presented structures, it is concluded that these represent the enzymatically active R state conformer. A mechanism for the deaminase reaction is proposed. It comprises steps to open the pyranose ring of the substrate and a sequence of general base-catalyzed reactions to bring about isomerization and deamination, with Asp72 playing a key role as a proton exchanger.

Structure 15 December 1995, **3**:1323–1332

Key words: aldose-ketose isomerase, α/β open structure, allosteric enzyme, NAD-binding domain

Introduction

The enzyme glucosamine 6-phosphate deaminase (GlcN6P deaminase, E.C. 5.3.1.10) catalyzes the reversible isomerization and deamination of D-glucosamine 6-phosphate (GlcN6P) into D-fructose 6-phosphate (Fru6P) and ammonium ion [1–3]. This enzyme has been identified in several animal, fungal and bacterial species and completely purified to homogeneity from *Escherichia coli* [3], *Candida albicans* [4] and dog kidney [5]. The gene encoding the enzyme has been cloned from both *E. coli* [6] and *C. albicans* [4]. In *E. coli*, GlcN6P deaminase is an allosteric enzyme, activated by *N*-acetyl-D-glucosamine 6-phosphate (GlcNAc6P). It catalyzes a step in the catabolism of amino sugars, that allows bacteria to utilize glucosamine (GlcN) or *N*-acetyl-D-glucosamine (GlcNAc) from the medium as sources of carbon. Amino sugars are also components of lipopolysaccharide and proteoglycan that form the bacterial cell wall. When no amino sugars are available, GlcN6P is formed from Fru6P and L-glutamine by the enzyme GlcN6P synthase. The enzymes involved in these anabolic and catabolic reactions are carefully regulated [7]. The proteins which participate in the transport and utilization of GlcNAc by *E. coli* are encoded by the genes of the divergent operons *nagE* and *nagBACD* [8,9]. These genes are expressed when the bacterial cells grow on GlcN or GlcNAc; the induction is mediated by GlcNAc6P which binds to the product of the *nagC* gene — a repressor protein. GlcNAc6P, the co-inducer of the regulon, is also the allosteric activator of GlcN6P deaminase, the product of the *nagB* gene. This enzyme, therefore, plays a central role in the regulated balance of amino sugar synthesis and utilization due to its allosteric properties.

GlcN6P deaminase is a hexameric protein composed of identical subunits of 266 residues whose sequence is known from its encoding gene. A systematic search for sequence homology did not reveal significant similarity with any other protein, except with GlcN6P deaminases from other species [10]. The enzyme from *E. coli* has been purified from an overproducing strain [11] and the kinetics of its allosteric activation have been studied in detail [12]; it displays homotropic cooperativity towards its substrates GlcN6P and Fru6P in the forward and reverse directions of the reaction, respectively. These homotropic kinetics can be accurately described by the concerted allosteric model of Monod *et al.* [13] for the case of non-exclusive binding of the substrate. The allosteric activator, GlcNAc6P, is an exclusive-binding ligand, which has the effect of increasing the apparent affinity of the enzyme for GlcN6P (or Fru6P in the reverse reaction), with accompanying loss of homotropic

*Corresponding author. Present addresses: †Departamento de Física e Biofísica, IB-UNESP, Botucatu, CP 510, 18618–000, Brazil. ‡Departamento de Reconocimiento Molecular y Bioestructura, Instituto de Biotecnología, Universidad Nacional Autónoma de México, PO Box 510-3, Cuernavaca, MOR, 62250, México.

 ISSN 0969-2126

cooperativity. At saturating concentrations of GlcNAc6P, GlcN6P deaminase displays hyperbolic kinetics. This kind of allosteric behaviour characterizes the K-systems [13].

GlcN6P deaminase belongs to the (2-*R*) aldose-ketose isomerase class of proteins. Enzymes from this group catalyze the removal of one hydrogen from C2 of the aldose and add back a hydrogen to the C1 of the ketose (or the opposite in the reverse reaction) going through a *cis*-enediol intermediate. The prochiral position to which tritium is transferred at the ketose C1, has been determined using isotope-exchange experiments for several aldose-ketose isomerases [14], including GlcN6P deaminase [15,16]. In all cases a general pattern was found, with a *cis*-enediol intermediate and a suprafacial proton abstraction and transfer along one side of the plane of the enediol, catalyzed by a single basic group on the enzyme.

Two special cases in this class are GlcN6P deaminase and GlcN6P synthase which are both aldose-ketose isomerases and amino transferases. Midelfort and Rose [15] found a low amount of intramolecular tritium transfer from C2 of GlcN6P to C1 of Fru6P (0.7% in single turnover measurements). This was taken as evidence that the deaminase has a mechanism similar to other aldose-ketose isomerases [17]. A low rate of intramolecular tritium transfer was also found in the reaction catalyzed by *E. coli* GlcN6P synthase [18]. Some modifications of this general mechanism have been found subsequently. One of the best known enzymes from this class is triosephosphate isomerase (TIM). In addition to the carboxylate which participates in the enolization reaction, TIM has a second base, the unprotonated imidazole from His95, which polarizes the carbonyl group of the substrate and transfers a proton to the enediolate intermediate [19].

An interesting exception in the class of aldose-ketose isomerases, is D-xylose isomerase, which does not have a proton transfer mechanism catalyzed by a basic group at the active site, but a hydride ion is transferred directly [20,21]. In these examples, knowledge of the enzyme structure from crystallographic data was of great value in elucidating the mechanism of the catalyzed reaction.

In a previous report [22], we described the crystallization of GlcN6P deaminase from *E. coli* and presented the preliminary X-ray diffraction analysis of the crystals obtained with phosphate salts as precipitating agents. The crystals belong to space group R32, with cell parameters a=b=125.9 Å, c=223.2 Å. These crystals have two monomers of 266 residues each in the asymmetric unit, with a solvent content of 52%. A complete data set to 2.1 Å resolution was collected from one crystal using synchrotron radiation and an image-plate detector.

In the present study, we present the crystallographic structure of *E. coli* GlcN6P deaminase in three different complexes. One of them is the complex obtained in the previously reported crystals [22], with two inorganic phosphate ions per monomer, bound to what were later identified as the allosteric and active sites, named sites I and II respectively. This complex will be referred to here as the enzyme–2Pi complex. Two more complexes were studied, in which the allosteric activator, GlcNAc6P, or the competitive inhibitor, 2-deoxy-2-amino D-glucitol-6-phosphate (GlcNol6P) [12,15], were bound to sites I and II. In the enzyme–activator–Pi complex, the allosteric activator is bound to site I and inorganic phosphate is bound to site II. In the enzyme–inhibitor–Pi complex, GlcNol6P is present at site II and inorganic phosphate is bound at site I. Site I is thus identified as the allosteric site and site II as the catalytic site. The catalytic mechanism of the reaction catalyzed by GlcN6P deaminase is discussed in the context of previous experimental evidence and the known mechanisms for other aldose-ketose isomerases.

Results and discussion

Crystallographic structure determination and refinement

The structure of the enzyme–2Pi complex was solved by the double isomorphous replacement method (MIR) with no anomalous dispersion data. Two successful derivatives were produced, one using the platinum compound K_2PtCl_4 and the second using mersalyl acid, a mercury organometallic compound. The platinum derivative diffraction data extended to 2.5 Å resolution and the crystals were stable enough to allow a long data collection, providing a data set of high quality which is almost complete to 2.5 Å resolution (Table 1). All tested mercury derivatives caused reduced crystallinity and increased radiation sensitivity of the crystals, albeit to differing extents. It was possible, however, to collect a 74% complete data set to 3.0 Å resolution from a crystal briefly soaked in a low concentration mersalyl acid solution. The heavy-atom sites were found by combining Patterson vector superposition methods and cross-phase difference Fourier maps. Six out of the seven platinum sites and four out of the five mercury sites were related by a single local twofold axis oriented identically to the twofold axis determined previously by the self-rotation function analysis [22]. The resulting 3 Å resolution MIR map showed clear molecular boundaries. Solvent-flattening techniques, as implemented by Leslie [23,24], were used to refine the MIR phases to 3 Å and to extend the phasing by breaking the phase ambiguity of the single

Table 1. Data collection statistics.

	Enzyme–2Pi	Mersalyl acid	K_2PtCl_4	Enzyme–activator–Pi	Enzyme–inhibitor–Pi
Resolution (Å)	2.1	3.0	2.5	2.5	2.5
Unique reflections	38368	10327	22611	20036	18437
Completeness (%)	97.4	74.0	95.5	88.1	81.1
Multiplicity	5.2	2.2	2.3	1.7	1.7
R_{merge} (%)*	10.1	9.0	8.2	5.1	6.9
R_{deriv} (%)†	–	16.3	26.8	–	–
Number of sites	4	5	7	2+2	2+2

*$R_{merge}=\sum_h\sum_i|I_{hi}-\langle I_h\rangle|/\sum_h\langle I_h\rangle$. †$R_{deriv}=\sum_h||F_{PH}(h)|-|F_P(h)||/\sum_h|F_P(h)|$.

isomorphous replacement (SIR) platinum derivative data in the range 3–2.5 Å. The polypeptide chain could be readily traced in the final map and the excellent correspondence between the electron densities for the two independent molecules in the asymmetric unit made it unnecessary to further refine the phases by symmetry averaging. Chain tracing was conducted in one of the monomers, although always keeping the electron-density map from the other monomer superimposed on the graphics screen. From the solvent-flattened 2.5 Å MIR map it was possible to identify unambiguously 230 of the 266 residues of the monomer. The missing residues were from the loop comprising residues 78–85, the chain segment between residues 161–182 and the eight residues at the C terminus of the molecule. Careful inspection of the molecular envelope at this stage indicated that the automatic envelope determination procedure employed [23] had excluded density regions corresponding to the missing segments. Using the original 3 Å MIR map to guide the tracing, the remaining parts of the chain could be traced with the exception of the C-terminal octapeptide, which is highly disordered. It was only in the final stages of the refinement that the density associated with the C terminus was found. Two phosphate ions per monomer were detected at this stage, being the strongest peaks of the electron-density map.

The final model includes two complete and independently refined monomers (2×266 residues), four phosphate ions and 348 water molecules, has an R factor of 17.4% (for all data to 2.1 Å resolution) and root mean square deviations (rmsds) from ideal geometry of 0.006 Å for bond lengths, 1.3° for bond angles and 23.7° for torsion angles (Table 2).

Table 2. Refinement statistics.

	Enzyme–2Pi	Enzyme–activator–Pi	Enzyme–inhibitor–Pi
Final R (%)	17.4	16.1	16.5
Rfree (%)	22.4	21.2	22.5
Water molecules	348	189	216
Rmsd bonds (Å)	0.006	0.005	0.005
Rmsd angles (°)	1.30	1.33	1.32
Rmsd dihedrals (°)	23.70	23.80	23.95

Monomer structure and chain topology

The monomer fold is a typical open α/β structure dominated by a central seven-stranded parallel β sheet with topology 4x, 1x, 1x, −3x, −1x, −1x [25], surrounded on both sides by eight α helices and a two-turn 3_{10} helix (Fig. 1). The helices have been numbered sequentially from 1–8 and the sheet strands from A–G. Strand C continues at its C terminus to form part of a second antiparallel β sheet with topology 2, −1, with strands named A′, B′, C′ (Fig. 1a). Helix 5, placed in sequence between strands B′ and C′, is highly flexible and makes very few contacts with the rest of the molecule (Fig. 1b). Helix 4, which is hydrophilic, is also only loosely connected, having Cys118 and Tyr121 as the sole contacts with the remainder of the structure. Overall, the topology of the monomer of GlcN6P deaminase (Fig. 1a) resembles an NAD-binding domain modified by the addition of three segments: the N-terminal sequence up to residue 35; the C terminus (residues 243–266); and the segment including amino acids 141–188. The remainder of the polypeptide presents a folding pattern which resembles a typical dinucleotide-binding structure. The N-terminal addition forms strand A and helix 1. Unusually for parallel sheets in open α/β structures, the first strand, strand A, is positioned at the edge of the β sheet rather than towards its centre [26]. This strand contains the N terminus which participates in the formation of the allosteric site of the hexamer (see below). A second addition is formed by the segment 141–188, which contains a loop involved in the catalytic mechanism (discussed below) and also a motif formed by strand B′, helix 5 and strand C′. Strands B′ and C′ form part of the antiparallel β sheet. Residues 158 and 160 in strand B′ are part of the allosteric site of the enzyme, while in helix 5, Arg172 is one of the substrate-binding residues. The C terminus contains two additional structures, the loop 243–250, involved in intersubunit contacts, and helix 8. A superposition of the 35 Cα atoms in the six parallel strands (excluding strand A) with the corresponding atoms of the NAD-binding domain of glyceraldehyde-3-phosphate dehydrogenase resulted in an rmsd of 2.2 Å, which is similar to values obtained for superpositions between other NAD-binding domains.

Two bound phosphate ions were identified per monomer in this structure. One of them is salt-linked to Lys208 and Arg172 and is also connected through hydrogen bonds to the loop formed by residues 40–44. The other phosphate is placed in the interface between two monomers and is bound through salt bridges to Arg158, Lys160 and the N-terminal amino group of a neighbouring monomer. This second phosphate is also hydrogen-bonded to the main-chain nitrogen from residue 152 and the Oγ from Ser151.

Hexamer structure

The crystal structure presents the chains grouped in hexamers, with interhexameric interactions that are much weaker than those amongst monomers internal to each hexamer. This observation is consistent with the experimental evidence demonstrating that the active form of *E. coli* GlcN6P deaminase is a hexamer with high thermal stability [3] as shown by high-sensitivity scanning calorimetry experiments [27]. The hexamer (Fig. 2), which can be described as a dimer of trimers, has a threefold crystallographic axis and three twofold axes perpendicular to the threefold axis and crossing it at the centre of the particle. This results in internal 32 symmetry. The twofold axes are non-crystallographic in this structure [22].

The hexamer has a central cavity which communicates with the external solvent. The unique intersubunit contacts are built close to the threefold axis and to each of

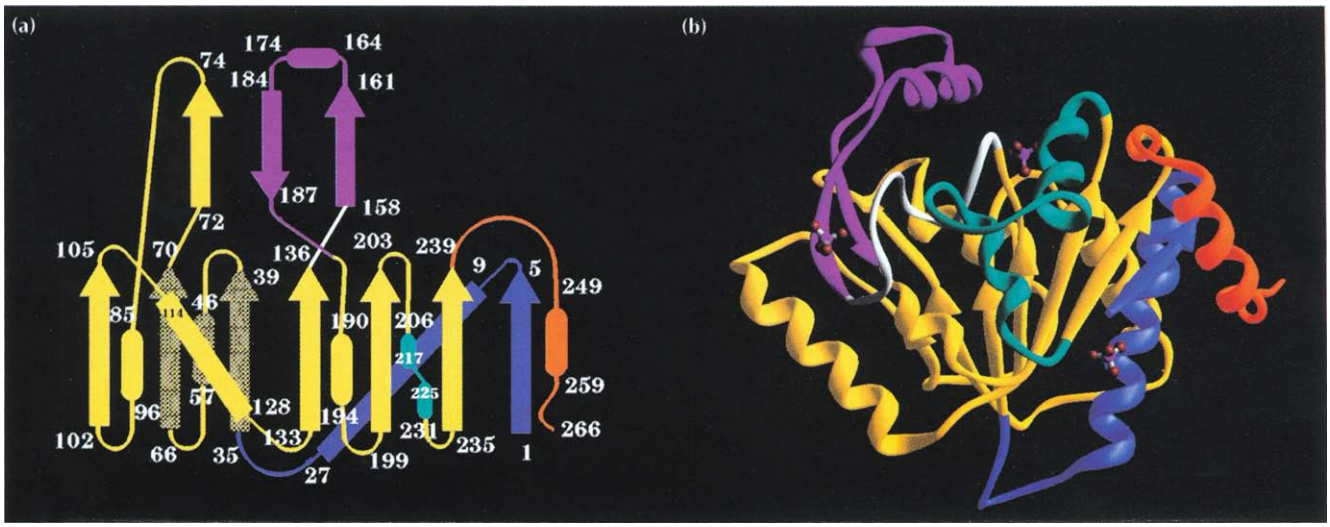

Fig. 1. GlcN6P deaminase monomer. **(a)** Topology diagram. A central seven-stranded parallel β sheet (DCBEFGA) surrounded by helices 1–8 forms a typical open α/β structure together with an antiparallel three-stranded β sheet (A'C'B') at the top of the figure. **(b)** Ribbon diagram. The colour coding is as follows: yellow, secondary structures with homology to NAD-binding domains; blue, 35-residue addition to the N terminus; orange, a C-terminal addition; cyan, an α helix/loop/3_{10} helix motif equivalent to an α helix in a typical NAD-binding domain and responsible for the intersubunit contacts close to the threefold axis; white, a loop containing catalytic residues; magenta, a βαβ motif which, together with the loop in white, constitutes an insertion in the NAD-binding domain. In (b), three phosphate ions are shown in ball-and-stick representation. The central one is at the active site and the two flanking phosphates occupy the symmetry-related allosteric sites in contact with the monomer shown.

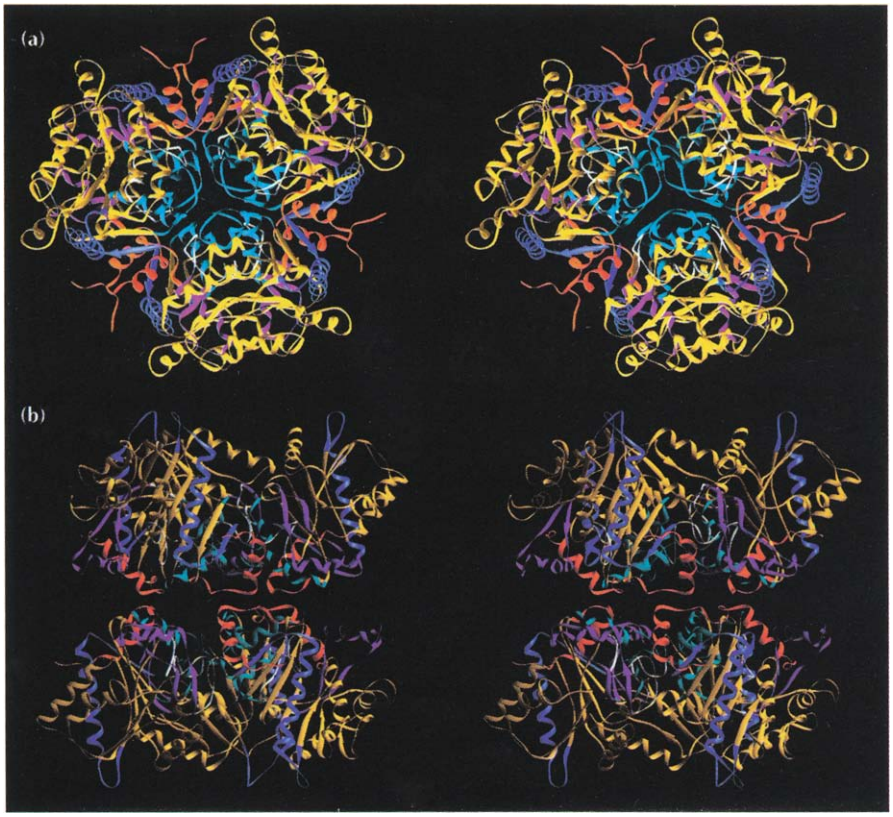

Fig. 2. Two views of the hexamer. The chain segments are colour coded as in Figure 1. **(a)** View along the threefold axis, with the three twofold axes in the plane of the figure. **(b)** The threefold axis is parallel to the plane of the figure.

the three twofold axes. Thiol groups from Cys219 and its two symmetry-related equivalents are close to the threefold axis and appropriately positioned for a disulphide bridge to form between two of them, by rotating one Sγ atom around the bond Cα–Cβ. In a previous chemical study of the cysteine residues of this enzyme, it was shown that the sulfhydryl group from Cys219 behaves as if it were oxidized, forming interchain disulphide bridges [28]. In a mutant form of the deaminase in which all the cysteines (except for Cys219) were replaced by serine, dissociation by denaturing agents under non-reducing conditions, always resulted in a mixture of monomers

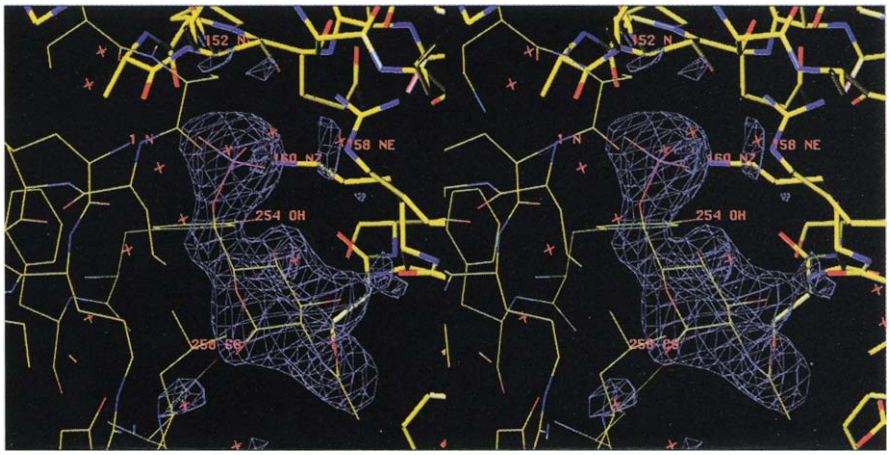

Fig. 3. Stereoview of the difference density for the refined structure of the allosteric activator, GlcNAc6P, in the enzyme–activator–Pi complex. The activator is bound in the allosteric site between two monomers, which are distinguished by different bond thicknesses.

and dimers [28]. The structure proposed here is consistent with these results. This particular arrangement of Cys219 is not significant either for the stability of the hexameric protein nor for its function. This conclusion comes from the study of the site-directed mutant Cys219→Ser, which is a stable hexamer and is not significantly altered in either catalytic or allosteric properties [28]. A similar arrangement of cysteines around a symmetry axis, a fivefold axis in this case, was found in the structure of the foot-and-mouth disease virus. In this structure it was also found to be non-functional [29].

Other intersubunit contacts close to the threefold axis include interactions between residues from the loop 216–223 which contains Cys219 and residues 230–232 from the 3_{10} helix. These interactions involve hydrogen bonds and van der Waals contacts, forming a core which stabilizes the trimeric structure.

The interactions between two trimers to form the hexameric particle are restricted to contacts which are close to the non-crystallographic twofold axis. Residues 244–250 (Figs 1,2) from two related monomers are in close contact through six intersubunit hydrogen bonds. This segment contains three different structural elements: residues 244 and 245 form the C-terminal end of a short 3_{10} helix; residues 246 and 247 form a short antiparallel β sheet with the corresponding symmetry-related residues in the other monomer; and residues 248–250 form the N terminus of helix 8. In this way the C-terminal end of a 3_{10} helix interacts with the N terminus of an α helix of the neighbouring monomer. These intersubunit contacts are strengthened by the presence of salt bridges between Glu246 and Lys250, from each subunit.

Enzyme–activator–Pi complex: the allosteric site

Co-crystallization of GlcN6P deaminase and its allosteric activator was performed in phosphate buffer, and the resulting crystals are isomorphous to those obtained in the absence of GlcNAc6P. Difference Fourier maps show electron density concentrated at the interface between two monomers, with no other peaks larger than 3.0σ. A molecule of the allosteric activator was easily built in this density. Figure 3 shows the density of the refined GlcNAc6P molecule (see refinement procedure in the Materials and methods section; statistics in Table 2). The phosphate moiety of the bound activator is located in the same place as the inorganic phosphate ion present in the enzyme–2Pi structure [22].

Kinetic evidence shows that GlcNAc6P, the allosteric activator of GlcN6P deaminase, is an exclusive-binding ligand (i.e. it binds only to the R conformer, which is the species of the enzyme with high affinity for its substrate [3,12]). From the difference Fourier maps and taking into account these kinetic considerations, it follows that the protein conformation present in the enzyme–2Pi and enzyme–activator–Pi complexes corresponds to the R allosteric state. We have recently crystallized the enzyme without ligands using sodium acetate as precipitant (EH, MMA, MLC and GO, unpublished data). In this structure, which represents the inactive T-state conformer, each monomer is rotated by 11° around an axis parallel to the threefold axis. The allosteric site, because of its location at the intersubunit interface, is totally distorted as a result of this rotation. Inorganic phosphate is known to be inhibitory at high concentrations (K_i=50 mM). The structure of the enzyme–2Pi complex provides evidence that, at very high concentrations (1.2 M), phosphate induces the allosteric transition from the T to the R state.

The observed electron density for the activator clearly shows that the bound sugar is the α-anomer. As no special steric hindrance with the enzyme prevents binding of the β-GlcNAc6P, this preference is probably due to the internal close contacts between the *N*-acetyl moiety and the O1 in the β-anomer.

The phosphate moiety of the activator is bound in the same position as the inorganic phosphate in site I in the enzyme–2Pi complex and therefore has the interactions described in the monomer structure section. The O3 atom in the sugar moiety is hydrogen bonded to the backbone carbonyl of residue 159. The hydrophobic part of the acetyl moiety is in van der Waals contact with Leu159. Other alcohol groups of the activator are hydrogen bonded to crystallographic water molecules.

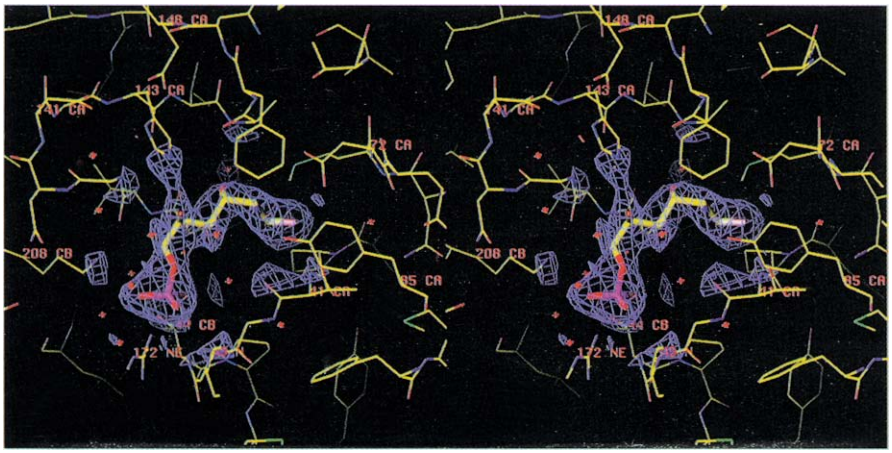

Fig. 4. Stereoview of the active site of GlcN6P deaminase. The density corresponds to the dead-end inhibitor in the refined structure of the enzyme–inhibitor–Pi complex. A number of functional amino acids are shown. In the binding site for the phosphate moiety, Arg172 (bottom), Lys208 (left) and the loop 40–45 (right) are shown.

Enzyme–inhibitor–Pi complex: the active site

The enzyme was co-crystallized with the competitive, dead-end inhibitor GlcNol6P. Its inhibition constant is three orders of magnitude lower than the K_m for the substrates GlcN6P and Fru6P. This low K_i is considered reasonable evidence for GlcNol6P bearing structural similarity with a transition-state intermediate of the reaction [15].

Crystals were obtained in the presence of 0.8 M phosphate and 0.45 mM GlcNol6P. The structure shows the inhibitor bound with its phosphate moiety placed in one of the phosphate-binding sites of the enzyme–2Pi complex structure, unequivocally identifying it as the active site. The molecule in its density after refinement (see the Materials and methods section for details and Table 2 for statistics) is shown in Figure 4. This site appears in a crevice formed by two loops situated at the C termini of strands B and E of the parallel sheet. This position is in accordance with the criteria for binding site location in NAD-binding domains and more generally for α/β proteins with doubly-wound open β sheets [30]. The loop composed of residues 41–44, placed between strand B and helix 2, forms hydrogen bonds with the phosphate moiety of the inhibitor (Fig. 4). Topologically, this corresponds to the phosphate-binding loop in NAD-binding domains. Other interactions of the phosphate moiety involve the Nζ from Lys208 situated at the N terminus of helix 7, and Nη of Arg172 located within helix 5 (residues 163–175). This is the closest contact that helix 5 makes with the remainder of the structure. The enzyme–inhibitor–Pi complex also presents a phosphate ion bound at the allosteric site identical to the enzyme–2Pi complex. The inhibitor appears bound in an extended conformation with the O5 atom pointing towards Nε2 of His143. This histidine residue is in contact via Nδ1 with Oδ1 of Asp141 (2.9 Å) and Oε1 of Glu148 (3.1 Å) (Fig. 4) in an arrangement that resembles the proton-relay system present in many enzymes [31] but with an additional acidic group in its neighbourhood. Another outstanding aspect of the inhibitor-binding site is the position of Asp72, which lies oriented towards the hydrogen on C2 (Fig. 4) and with its Oδ2 atom forming a hydrogen bond (2.9 Å) with O1 of the inhibitor. An acidic residue is totally conserved at this position in NAD-binding domains, where it forms part of the ribose-phosphate binding site. The orientation of Oδ1 with respect to the C2 atom of the inhibitor will be related to the catalytic mechanism (see below).

The refinement of all structures described in this paper produced the same main-chain conformation, within experimental error (Table 3).

Table 3. Rmsds (in Å) for Cα atoms in the different complexes.

	Enzyme–2Pi	Enzyme–activator–Pi	Enzyme–inhibitor–Pi
Enzyme–2Pi	0.260	0.122	0.137
Enzyme–activator–Pi		0.270	0.133
Enzyme–inhibitor–Pi			0.253

The differences between the two monomers in the asymmetric unit appear in the diagonal.

Previous kinetic studies of the GlcN6P deaminase demonstrated that saturating concentrations of the allosteric activator or the dead-end inhibitor entirely displace the allosteric equilibrium towards the R conformer [10]. According to the evidence gained from studies of the enzyme in solution, it is possible to conclude that the crystallographic structures described here correspond to the R allosteric conformer. The R form has a higher affinity for the substrate, GlcN6P, and is the only form able to bind GlcNAc6P [12]. Our results also prove that inorganic phosphate can be bound both to allosteric and active sites. It has been observed that high concentrations of inorganic phosphate competitively inhibit GlcN6P deaminase (with a K_i of 50 mM with respect to GlcN6P, at pH 7.7 and in the presence of a saturating concentration of GlcNAc6P), whilst homotropic cooperativity decreases (MMA and MLC, unpublished data). The loss of cooperativity may be explained by the homotropic activation of the enzyme. The present results clearly indicate that inorganic phosphate is also a ligand of the allosteric site, and that it stabilizes the R conformer of the enzyme by serving as both homotropic and

heterotropic ligand. This also shows the key role of the phosphate-binding groups of the protein, which appear to be the only ones relevant for the allosteric function.

The catalytic mechanism

Analysis of the complex containing GlcNol6P bound to the active site of GlcN6P deaminase provides insight into the enzyme's reaction mechanism. GlcNol6P is kinetically a linear competitive inhibitor, and its K_i is three orders of magnitude lower than the K_m for GlcN6P or Fru6P. One explanation for this difference in affinity is that the enzyme binds the aldehydo form of GlcN6P exclusively. Indeed, Midelfort and Rose have shown the absolute specificity of GlcN6P deaminase for the α-anomer of GlcN6P [15]. Ring-opening steps must then be considered in the overall reaction mechanism giving Fru6P from the pyranose form of a GlcN6P. We thus built a model of the pyranose form of the substrate, just superimposing the phosphate moiety and the atoms C6, C5, C4 and O5 of the crystallographic inhibitor conformation with those of the substrate. This model had no unacceptably close contacts with the protein and was stable after energy minimization. The modelled molecule of the substrate bound to the active site in its pyranose form shows that its O5 atom, which is part of the pyranose ring, is in close contact with Nε2 of His143 (as the modelled substrate structure is superimposed with the inhibitor at this atom, this contact can be observed in Fig. 4). This residue has two acidic groups, from Asp141 and Glu148, in contact with its Nδ1 atom. This arrangement could be important for the catalysis of the ring-opening step of the reaction. A histidine positioned similarly with respect both to the modelled substrate and to a carboxylic side chain has been found in the crystallographic structure of D-xylose isomerase and related therein to the mechanism of the ring-opening reaction [21].

In its closed conformation, the model shows that the GlcN6P amino group is in close contact with Asp72. This arrangement could stabilize a negative charge on the aspartic carboxylate and a positively charged ammonium group on the substrate. Once the substrate ring is opened, it is expected to adopt a binding conformation similar to that of the competitive inhibitor, GlcNol6P, in which Asp72 is appropriately positioned to abstract the hydrogen at C2 of the substrate. The subsequent steps for the conversion of the aldehydo-GlcN6P to Fru6P are shown in Figure 5. The carboxylate group from Asp72 catalyzes the enolization of the amino sugar by removing the C2 hydrogen from aldehydo-GlcN6P to give a *cis*-enolate-ammonium intermediate (III in Fig. 5). The latter takes the proton from Asp72 onto the O1 oxygen to form the corresponding enol-ammonium (IV in Fig. 5). There are two possible ways to achieve the next step. The

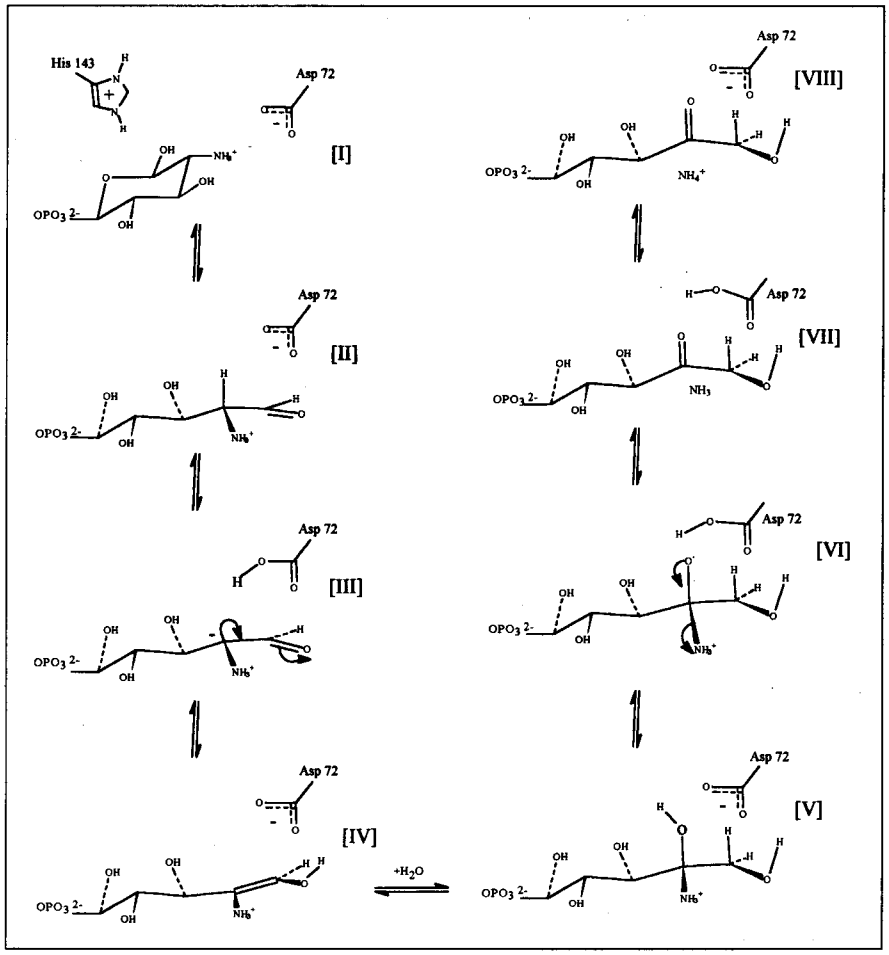

Fig. 5. Catalytic mechanism for GlcN6P deaminase. The mechanism proceeds via the following five steps. 1. The pyranose ring of the substrate is catalytically opened, as described (see text). 2. The substrate is bound with its amino group protonated (II). The enzyme-bound GlcN6P is enolized by the uptake of the hydrogen atom from C2 by Asp72 (III). 3. A *cis*-enol-ammonium intermediate is formed. The proton at Asp72 is then transferred to the oxygen at C1, which in the inhibitor complex, is hydrogen bonded to the aspartate (IV). 4. A water molecule reacts in one of the two pathways described (see text) to form the intermediate V. 5. The previous intermediate loses the proton of the hydroxyl in C2 which is again taken by Asp72 (VI). In a concerted way, the ammonium group is lost as ammonia (VII). Kinetic evidence indicates that ammonium ion rather than ammonia is the true substrate of the reverse reaction of GlcN6P deaminase [29]. We propose that Asp72 donates this proton to generate the ammonium ion (VIII).

proton from the ammonium group could again be transferred to the Asp72 carboxylate. The resulting *cis*-enol-amine then removes the proton from Asp72 to the position C1 pro-*R* of the intermediate which rearranges to form fructosimine 6-phosphate. The imino bond reacts with a water molecule, giving an unstable carbinol ammonium intermediate (step V in Fig. 5). Alternatively, the π-bond (C1–C2) of the *cis*-enol-ammonium is attacked by a water molecule coming from the *re*-face of the intermediate (i.e. from the same side as Asp72).

The newly formed intermediate (step V in Fig. 5) has a structure which resembles that of the competitive inhibitor GlcNol6P and is expected to be very unstable, decomposing into Fru6P and ammonia. In this step, a proton is transferred to the Asp72 carboxylate (step VI to step VII in Fig. 5). The kinetic study of the reverse reaction of *E. coli* GlcN6P deaminase revealed that ammonium ion and not ammonia is the true substrate of the enzyme (MLC and MMA, unpublished data). It is then expected that ammonia formed in this reaction is released as ammonium ion, taking a proton from Asp72. There is no experimental evidence for enzyme-catalyzed ring closure of the Fru6P formed by this reaction. This aspect of the mechanism will require more experimental work before it will be understood fully.

Steps II and III of this proposed mechanism (summarized in Fig. 5) coincide with the proposed mechanism for the His95→Gln mutant form of TIM [32]. It is interesting to note that in this mutant TIM, the geometry relating the enol intermediate (in this case a *cis*-enediol) to the carboxylate of Glu165 is essentially identical to that found for the equivalent group of Asp72 in the R conformer of GlcN6P deaminase (Fig. 4).

Biological implications

We report here the structure determination of the hexameric enzyme glucosamine 6-phosphate (GlcN6P) deaminase. This enzyme catalyzes the conversion of D-glucosamine 6-phosphate (GlcN6P) into D-fructose 6-phosphate and ammonium ion and is the first enzyme involved in the metabolism of amino sugars to have its structure solved. The reaction catalyzed by GlcN6P deaminase is a unique example of an aldose-ketose isomerization coupled with a deamination. GlcN6P deaminase is mechanistically related to other aldose-ketose converting enzymes. Nevertheless, its fold differs from that of other enzymes in this group, such as triosephosphate isomerase [33], phosphoglucose isomerase [34] and xylose isomerase [21]. Similarities in geometry of the active site of GlcN6P deaminase with xylose isomerase or triosephosphate isomerase may reflect convergent evolution.

GlcN6P deaminase is an allosteric enzyme and kinetic evidence shows that it undergoes a concerted allosteric transition. Nevertheless, some site-directed mutants studied recently exhibit a more complex allosteric behaviour, such as non-concerted activation and a mixed effect on K_m and K_{cat} [12]. The current knowledge about the kinetics of this enzyme, and its easy expression and purification, indicate that GlcN6P deaminase may be a useful system for the study of allosteric transitions.

The structure of the complex formed by the enzyme with its competitive inhibitor, 2-deoxy-2-amino D-glucitol-6-phosphate, gives insight into the catalytic mechanism of the enzyme. It has allowed us to propose a reaction mechanism that is somewhat different to that described previously for related enzymes [14], in particular with respect to steps involving uptake of water and loss of ammonia.

Despite the lack of significant sequence similarity, the structures presented here reveal that GlcN6P deaminase is topologically related to the NAD-binding domains. The finding that its allosteric site and the intersubunit interactions involve chain segments that are part of the insertions to the NAD-binding domain core, suggests that both types of polypeptides may be derived from a common ancestor.

Materials and methods

Enzyme preparation and crystallization

GlcN6P deaminase from *E. coli* K12 from an overproducing strain was purified by allosteric site affinity chromatography as described [11]. Crystals were obtained by vapour diffusion in hanging drops at 20°C under the following conditions: for the enzyme–2Pi complex, in 1.33 M Na/K phosphate buffer pH 8.0; for the enzyme–activator–Pi complex, in Na/K phosphate buffer pH 8.2 plus 0.45 mM of GlcNAc6P; and for the enzyme–inhibitor–Pi complex, in Na/K phosphate buffer pH 8.2 plus 4.5 mM of GlcNol6P. The two last-mentioned crystals are isomorphous to those of the enzyme–2Pi complex, appear after 5 days and are completely grown within 21 days. The crystals are multifaceted and show variable morphology, growing up to 1.0 mm×0.6 mm×0.3 mm in size.

Data collection and preparation of heavy-atom derivatives

The native data set of the enzyme–2Pi complex was collected on the EMBL Protein Crystallography Station X31 in HASYLAB at DESY, Hamburg, using an image-plate detector, to a resolution of 2.1 Å, and processed using the MOSFLM package [35]. The structure of the enzyme–2Pi complex was solved by double isomorphous replacement. The heavy-atom derivative crystals were prepared by soaking in solutions of the mother liquor containing the heavy-metal salts: for the K_2PtCl_4 derivative the salt concentration was 1 mM and soaking time was 48 h; for the mersalyl acid, 0.1 mM and 24 h. Diffraction data sets for the isomorphous derivatives and activator and inhibitor complexes were collected on an R-AXIS IIC imaging plate area detector system (Rigaku International Co., Tokyo, Japan), mounted on a Rigaku RU200B rotating anode generator operating at 40 kV and 120 mA, fitted with a Cu target and graphite monochromator (λ=1.54178 Å). All crystals were cooled to 4°C to minimize radiation damage effects. The images

were processed with the software provided by the manufacturers of the equipment (Rigaku Co., manual No. ME201LR1). Details of all data collections are presented in Table 1.

Phase determination

The heavy-atom sites were located by vector superposition methods, as implemented in the program VECSUM of the CCP4 package [24], and were confirmed and placed on a common origin by cross-phase difference Fourier maps. The positions and occupancies of the heavy atoms were refined by a combination of real-space refinement (VECREF) and phased refinement (MLPHARE) with the CCP4 package. MIR phases were obtained to 3.0 Å with a figure of merit of 0.512 and the resulting electron-density map allowed the identification of a molecular envelope using the procedure of Leslie [23] implemented in the CCP4 package, adopting a local averaging radius of 8 Å and a solvent content of 50%. Solvent flattening was then used to improve MIR phases to 3 Å and to break the ambiguity in the K_2PtCl_4 SIR phases in the range 3–2.5 Å.

For the complexes of the enzyme with allosteric activator and inhibitor, initial phases were calculated from the refined enzyme–2Pi model.

Model building and crystallographic refinement

From the initial bones trace of the 2.5 Å solvent-flattened MIR map, Cα coordinates for 230 residues were assigned, using the program O [36]. The remaining residues were identified from the original 3 Å MIR map. The facilities for automatic main-chain and side-chain construction of the program O were used to complete the model, which was then manually adjusted to the density. The model was then duplicated to fit the density of the second monomer in the asymmetric unit, followed by crystallographic refinement with simulated annealing using the program X-PLOR [37], treating the two monomers independently. Water molecules were added at the final stages of the refinement. Isotropic individual B-factor refinement was carried out before and after water inclusion. The average values of the refined main-chain temperature factors, represented in the plot of Figure 6, indicate that residues 175–180 and the C-terminal hexapeptide are highly mobile in the crystal structure. Nevertheless, the electron-density map when contoured at the value of 1σ is compatible with the refined model in these regions. In all refinement steps 37741 independent reflections with $I>2\sigma(I)$ were employed, which represents 97.5% of the data in the resolution range 6.0–2.1 Å (86.6% in the shell 2.2–2.1 Å).

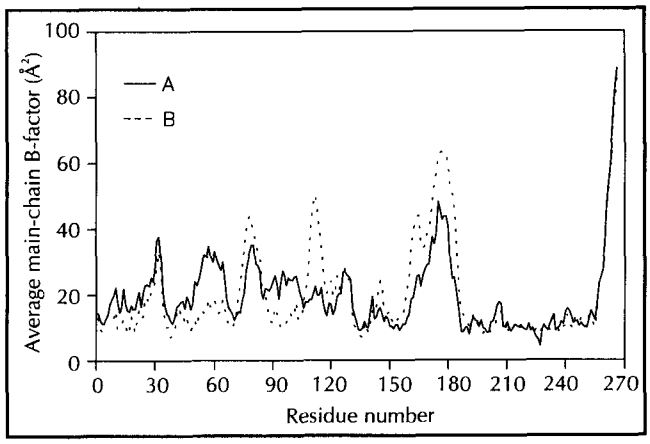

Fig. 6. Main-chain averaged B-factors. The values for the two independent monomers in the asymmetric unit are shown by full and dashed lines.

For the remaining complexes, the ligands were built into difference Fourier maps calculated using phases from the refined enzyme–2Pi model, excluding the phosphate ions and the water molecules. The refinement of the complexes, including the ligands, was also conducted using X-PLOR through positional and isotropic individual B-factor refinement, in order to allow for small conformational changes in the vicinity of the binding sites. Water molecules were also included in the final stages of the refinement in each case. Details of the statistics of the refinements are given in Table 2. Atomic contact quality analysis for the enzyme–2Pi complex using the program WHAT IF [38] resulted in a value of –0.52 which is close to the mean value for the 30 proteins chosen from the PDB to form the database. Three-dimensional profile analysis [39] resulted in a total score of 239 in concordance with the expected value for well determined proteins of the same length. The stereochemical quality of the main-chain dihedral angles resulted in a Ramachandran plot (not shown) with no residues in unfavourable regions.

The coordinates of the three complexes have been deposited in the Brookhaven Protein Data Bank with entry codes as follows: enzyme–2Pi complex (1DEA); enzyme–inhibitor–Pi complex (1HOR) and enzyme–activator-Pi complex (1HOT).

Acknowledgements: This work has received partial support from CNPq, FAPESP, CAPES and FINEP, which are hereby gratefully acknowledged. RCG and EH were supported by RHAE/CNPq, MLC and MMA also acknowledge the program PAPIIT (UNAM) and a grant from the European Commission.

References

1. Leloir, L.F. & Cardini, C.E. (1956). Enzymes acting on glucosamine phosphates. *Biochim. Biophys. Acta* **20**, 33–42.
2. Comb, D.G. & Roseman, S. (1958). Glucosamine metabolism. IV. Glucosamine 6-phosphate deaminase. *J. Biol. Chem.* **232**, 807–827.
3. Calcagno, M., Campos, P.J., Mulliert, G. & Suástegui, J. (1984). Purification, molecular and kinetic properties of glucosamine 6-phosphate isomerase-deaminase from *Escherichia coli*. *Biochim. Biophys. Acta* **787**, 165–173.
4. Nataranjan, K. & Datta, A. (1993). Molecular cloning and analysis of the Nag1 cDNA coding for glucosamine 6-phosphate deaminase from *Candida albicans*. *J. Biol Chem.* **268**, 9206–9214.
5. Lara-Lemus, R., Libreros-Minotta, C.A., Altamirano, M.M. & Calcagno, M.L. (1992). Purification and characterization of glucosamine 6-phosphate deaminase from dog kidney cortex. *Arch. Biochem. Biophys.* **297**, 213–220.
6. Rogers, M.J., Ohgi, T., Plumbridge, J.A. & Söll, D. (1988). Nucleotide sequences of the *Escherichia coli nagE* and *nagB* genes: the structural genes for the *N*-acetylglucosamine transport protein of the bacterial phosphoenolpyruvate sugar phosphotransferase system and for glucosamine 6-phosphate deaminase. *Gene* **62**, 197–207.
7. Plumbridge, J.A., Cochet, O., Souza, J.M., Altamirano, M.M., Calcagno, M.L. & Badet, B. (1993). Coordinated regulation of amino sugar-synthesizing and -degrading enzymes in *Escherichia coli* K-12. *J. Bacteriol.* **175**, 4951–4956.
8. Plumbridge, J.A. (1989). Sequence of the *nagBACD* operon in *Escherichia coli* K12 and pattern of transcription within the *nag* regulon. *Mol. Microbiol.* **3**, 506–515.
9. Vogler, A.P. & Lengeler, J.W. (1989). Analysis of the regulon from *Escherichia coli* K12 and *Klebsiella pneumoniae* and of its regulation. *Mol. Gen. Genet.* **219**, 97–105.
10. Altamirano, M.M., Hernández-Arana, A., Tello-Solís, S. & Calcagno, M.L. (1994). Spectrochemical evidence for the presence of a tyrosine residue in the allosteric site of glucosamine 6-phosphate deaminase from *Escherichia coli*. *Eur. J. Biochem.* **220**, 409–413.
11. Altamirano, M.M., Plumbridge, J.A., Hernández-Arana, A. & Calcagno, M. (1991). Secondary structure of *Escherichia coli* glucosamine 6-phosphate deaminase from amino acid sequence and circular dichroism spectroscopy. *Biochim. Biophys. Acta* **1076**, 266–272.
12. Altamirano, M.M., Plumbridge, J.A., Horjales, E. & Calcagno, M.L. (1995). Asymmetric allosteric activation of *Escherichia coli* glucosamine 6-phosphate deaminase produced by replacements of Tyr121. *Biochemistry* **34**, 6074–6082.

13. Monod, J., Wyman, J. & Changeux, J.P. (1965). On the nature of the allosteric transitions: a plausible model. *J. Mol. Biol.* **2**, 88–118.
14. Rose, I.A. (1975). Mechanism of the aldose-ketose isomerase reactions. *Adv. Enzymol.* **43**, 491–517.
15. Midelfort, C. & Rose, I.A. (1977). Studies on the mechanism of *Escherichia coli* glucosamine 6-phosphate isomerase. *Biochemistry* **16**, 1590–1596.
16. Walsh, C. (1977). *Enzymatic Reaction Mechanisms.* W.H. Freeman & Co., San Francisco, CA.
17. Rose. I.A. (1970). Enzymology of proton abstraction and transfer reactions. In *The Enzymes,* (2nd edn). (Boyer, P.D., ed.), vol. **2**, pp. 281–320, Academic Press, New York.
18. Golinelli-Pimpaneau, B., Le Goffic, F. & Badet, B. (1989). Glucosamine-6-phosphate synthase from *Escherichia coli*: mechanism of the reaction at the fructose 6-phosphate binding site. *J. Am. Chem. Soc.* **111**, 3029–3034.
19. Cleland, W.W. & Creevoy, M.K. (1994). Low-barrier hydrogen bonds and enzymic catalysis. *Science* **264**, 1887–1890.
20. Allen, K.N., Lavie, A., Farber, G.K., Glasfield, A., Petsko, G.A. & Ringe, D. (1994). Isotopic exchange plus substrate and inhibition kinetics of D-xylose isomerase do not support a proton-transfer mechanism. *Biochemistry* **33**, 1481–1487.
21. Blow, D.M., Collyer, C.A., Goldberg, J.D. & Smart, O.S. (1992). Structure and mechanism of D-xylose isomerase. *Faraday Discuss.* **93**, 67–73.
22. Horjales, E., *et al.*, & Oliva, G. (1992). Crystallisation and preliminary crystallographic studies of glucosamine 6-phosphate deaminase from *Escherichia coli* K12. *J. Mol. Biol.* **226**, 1283–1286.
23. Leslie, A.G.W. (1987). A reciprocal-space method for calculating a molecular envelope using the algorithm of B.C. Wang. *Acta Cryst. A* **43**, 134–136.
24. Collaborative Computational Project, Number 4 (1994). The CCP4 suite: programs for protein crystallography. *Acta Cryst. D* **50**, 760–763.
25. Richardson, J.S. (1981). The anatomy and taxonomy of protein structure. *Adv. Protein Chem.* **34**, 167–339.
26. Sternberg, M.J.E. & Thornton, J.M. (1977). On the conformation of proteins: the handedness of the connection between parallel beta-strands. *J. Mol. Biol.* **110**, 269–283.
27. Hernández-Arana, A., Rojo-Domínguez, A., Altamirano, M.M. & Calcagno, M.L. (1993). Differential scanning calorimetry of the irreversible denaturation of *Escherichia coli* glucosamine-6-phosphate deaminase. *Biochemistry* **32**, 3644–3648.
28. Altamirano, M.M., Plumbridge, J.A., Barba, H.A. & Calcagno, M.L. (1993). Glucosamine 6-phosphate deaminase from *Escherichia coli* has a trimer of dimers structure with three intersubunit disulfides. *Biochem. J.* **295**, 645–648.
29. Acharya, R., Fry, E., Stuart, D., Fox, G., Rowlands, D. & Brown, F. (1989). The three-dimensional structure of foot-and-mouth disease virus at 2.9 Å resolution. *Nature* **337**, 709–716.
30. Brändén, C.I. & Tooze, J. (1991). *Introduction to Protein Structure.* pp. 49–51, Garland Publ., Inc., New York and London.
31. Fink, A.L. (1987). Acyl group transfer: the serine proteases. In *Enzyme Mechanisms.* (Page, M.I. & Williams, A., eds), pp. 159–177, The Royal Society of Chemistry, London.
32. Komives, E.A., Chang, L.C., Lolis, E., Tilton, R.F., Petsko, G.A. & Knowles, J.R. (1991). Electrophilic catalysis in triose phosphate isomerase: the role of histidine-95. *Biochemistry* **30**, 3011–3019.
33. Banner, D.W., *et al.*, & Waley, S.G. (1975). Structure of chicken muscle triose phosphate isomerase determined crystallographically at 2.5 Å resolution using amino acid sequence data. *Nature* **255**, 609–614.
34. Shaw, P.J. & Muirhead, H. (1977). Crystallographic structure analysis of glucose 6-phosphate isomerase at 3.5 Å resolution. *J. Mol. Biol.* **109**, 475–485.
35. Wonacott, A.J., Dockerill, S. & Brick, P. (1985). *MOSFLM: A program for the measurement of integrated intensities on oscillation photographs.* Imperial College, University of London.
36. Jones, T.A., Zou, J.Y., Cowan, S.W. & Kjeldgaard, M. (1991). Improved methods for building protein models in electron density maps and the location of errors in these models. *Acta Cryst. A* **47**, 110–119.
37. Brünger, A.T., Kuriyan, J. & Karplus, M. (1987). Crystallographic R factor refinement by molecular dynamics. *Science* **235**, 458–460.
38. Vriend, G. (1990). WHAT IF: a molecular modeling and drug design program. *J. Mol. Graphics* **8**, 52–56.
39. Lüthy, R., Bowie, J.U. & Eisenberg, D. (1992). Assessment of protein models with three-dimensional profiles. *Nature* **356**, 83–85.

Received: **23 Jun 1995**; revisions requested: **12 Jul 1995**; revisions received: **29 Aug 1995**. Accepted: **5 Sep 1995**.